DOI: 10.1002/ejic.200600171

Semicarbazide-Functionalized Silicate Nanoparticles for Peptide Ligation

Tristan Doussineau,[b] Jean-Olivier Durand,[c] Ouafâa El-Mahdi,[a] Céline Maillet,[a] Oleg Melnyk,[a] Christophe Olivier,[a] and Monique Smaïhi*[b]

Keywords: Zeolites / Colloids / Peptides / Fluorescence spectroscopy / Organic–inorganic composites

Monodisperse silicate nanoparticles have been used for the development of a site-specific ligation method that enables the control of the biomolecule orientation at the solid–liquid interface. Two types of zeolite nanoparticles were studied: zeolite β, which possesses a Si/Al ratio of 25, and silicalite-1, which is a fully silicic material. Zeolite-type materials are microporous silicate with pores of a well-defined size ranging from 2 to 20 Å. Semicarbazide-functionalized silicate colloids have been prepared for the site-specific ligation of COCHO-modified polypeptides. The obtained colloidal suspensions have been characterized by complementary techniques providing information on the size distribution, morphology, and porosity of the particles and chemical nature of the grafting. The specificity of the particles' surface for the semicarbazide group has been studied by fluorescence spectroscopy with two peptides labeled with rhodamine. A first peptide bares a COCHO functionality, which should bind covalently with the semicarbazide surface. The second peptide bares an amine end-group, which should interact by nonspecific adsorption with the surface. The results demonstrated that the peptide/colloids' reactivity is dramatically influenced by the chemical composition of the particles' surface. Indeed, while zeolite β (aluminosilicate) particles react indifferently with the two peptides, silicalite particles (pure silicate) anchor exclusively the peptide bearing the COCHO functionality. This particular physisorption phenomenon of zeolite β is attributed to the aluminum atoms present at the particles' surface, which have a specific affinity for peptides.

Introduction

Nanoparticles (NPs) have great promise in bioanalysis and biotechnological applications because of their unique optical properties, high surface-to-volume ratio, and other size-dependent qualities.[1–3] When combined with surface modifications and composition control, these properties provide probes for highly selective and ultrasensitive bioassays.

The use of silica as a substrate in bioanalysis has a special advantage, as shown by its widespread use in biosensors and biochips. Silica can be synthesized by various preparation techniques to prepare NPs, transparent films, or solid flat materials.[4] Silica synthesis is governed by the chemical properties of the surface, which, in return, are based on the silanols and siloxanes present on the surface.[5] Silanol groups can be functionalized through different procedures.[6,7] Therefore, the versatility of silica in synthesis aspects as well as surface modifications offers a great advantage to the use of the materials in bioanalysis.

Among inorganic materials, the synthesis and studies of nanosized zeolites have attracted considerable attention in the last decade.[8] Zeolite-type materials are microporous silicate crystals with pores of a well-defined size ranging from 2 to 20 Å. This discrete pore system gives molecular sieve properties to these materials, which have found great utility as catalysts and sorption media. Lately, functionalized zeolite nanoparticles were envisaged for the preparation of controlled release capsules, artificial cells, chemical sensors, and adsorbents.

In many cases, covalent attachment of a biomolecule at the NPs' surface is preferred to avoid leaching of the biomolecules. The usual pathways for covalent attachment of biomolecules on silica surfaces consist of their functionalization by epoxides,[9] aldehydes,[10] or thiol groups.[11] However, as biomolecules usually possess more than one nucleophilic group, a random immobilization through multiple points of attachment is often observed.[12] Therefore, site-specific ligation methods are highly desired in order to control the biomolecule orientation at the solid–liquid interface.

Recently, we have described the preparation of α-oxo aldehyde (COCHO)- and semicarbazide-functionalized silica, for the site-specific ligation of hydrazinoacetyl- or COCHO-modified polypeptides.[13] Indeed α-oxo aldehyde peptides were shown to react chemoselectively and readily

[a] Biological Institute of Lille, UMR 8161 CNRS/Université de Lille 2/Institut Pasteur de Lille,
1 rue du Pr Calmette, 59021 Lille Cedex, France
E-mail: oleg.melnyk@ibl.fr
[b] IEM, UMR 5635 CNRS-ENSCM-UM2,
1919 route de Mende, 34193 Montpellier Cedex 5, France
E-mail: monique.smaihi@iemm.univ-montp2.fr
[c] Laboratoire de Chimie Moléculaire et Organisation du Solide, UMR 5637, case 007-Université Montpellier II,
Place Eugène Bataillon, 34095 Montpellier Cedex 5, France
Fax: +33-46714-3852
E-mail: durand@univ-montp2.fr

with the surface semicarbazide groups in very mild aqueous conditions. The α-oxohydrazone bond was readily formed and was very stable; no further reduction of the hydrazone bond was needed.

We have extended the α-oxo hydrazone chemistry to monodisperse silicate nanoparticles using α-oxo aldehyde peptides labeled with rhodamine. Two types of zeolite nanoparticles were studied: zeolite β and silicalite-1. Here, we describe the preparation of these nanoparticles, and their reactivity and selectivity for the covalent immobilization of COCHO-modified polypeptides.

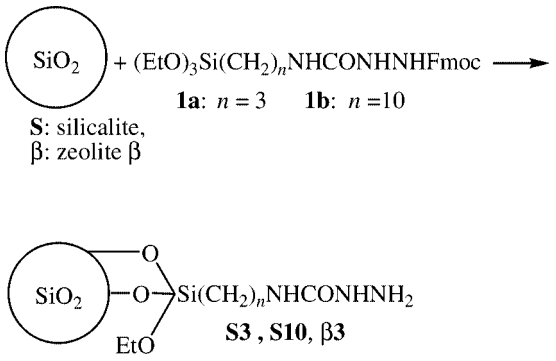

Scheme 1. Semicarbazide grafting chemistry (Fmoc: fluorenylmethoxycarbonyl).

Results and Discussion

Two types of samples have been used, differing mainly in their chemical composition: while silicalite is an "all-silica" zeolite, zeolite β contains aluminum atoms in its framework, with a Si/Al ratio that can be varied between 10 and 500. The zeolite β samples prepared in this study have a Si/Al ratio equal to 25.

As-synthesized zeolites contain an organic structure-directing agent (SDA) located in the framework channels. The SDA removal of zeolites through calcination is a common method employed to reveal the zeolite micropores, where the organic structure-directing agent is burned away. As-synthesized nanoparticles as well as template-free colloids have been used in this study as substrates for peptide ligation.

The anchoring of the peptides at the surface of these colloidal nanoparticles has been done in two steps. First, a semicarbazide coupling agent (SC) has been anchored at the colloids' surface followed by the grafting of peptides labeled with rhodamine. The specificity of the anchoring has been studied using two different peptides. One peptide molecule bares a COCHO functionality, which reacts covalently with the SC. The other peptide should only interact with the SC surface through physisorption, as it lacks the COCHO functionality.

Regardless of the zeolite framework and peptide used, stable colloidal suspensions were obtained for all samples. The different stages of the preparation procedure are presented in Scheme 1 and Scheme 2.

Subsequently, at each step of the preparation procedure, the size and morphology of the nanoparticles were studied by dynamic light scattering (DLS) and SEM. The influence of the various treatments on the porous characteristics of the samples has been analyzed by nitrogen sorption experiments.

^{29}Si and ^{13}C NMR were performed also at each step of the preparation procedure in order to characterize the surface bonding.

Finally, the specificity of the peptide anchoring was investigated by fluorescence spectroscopy.

The zeolite β and silicalite-1 nanoparticles are called **β** and **S**, respectively, in the following text, and the template-free silicalite and zeolite β nanoparticles are named tf-**S** and tf-**β**, respectively.

As indicated in Scheme 1, functionalization of zeolite **β** and silicalite **S** with silane **1a** leads to **β3** and **S3**, respectively. Alternatively, reaction of silanes **1** on template-free zeolite nanoparticles gives tf-**β3**, tf-**S3**, and tf-**S10**.

As indicated in Scheme 2, grafting of peptides **i** on nanoparticles of zeolite **β3** and silicalite **S3** leads to samples **β3-i** and **S3-i**.

Particle Size and Morphology

The DLS study performed after each step of the preparation procedure shows that the average diameter of the particles increases after the grafting procedure (Table 1, Fig-

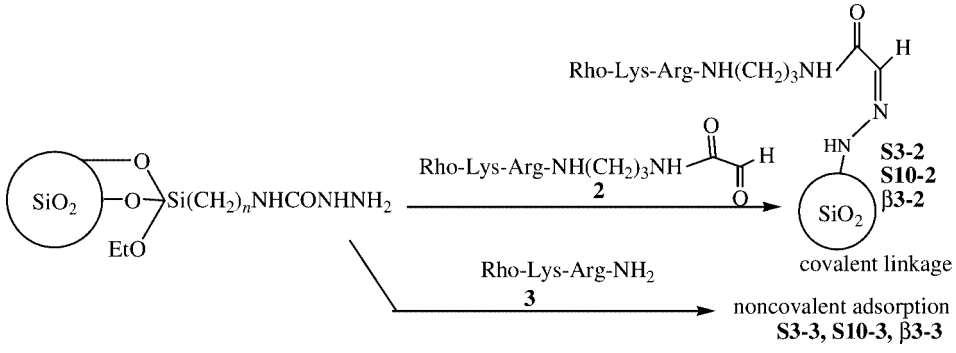

Scheme 2. Peptide grafting chemistry.

ure 1). According to the DLS measurements, the average particle sizes of the initial zeolite β and silicalite-1 nanoparticles are about 57 and 64 nm respectively. After functionalization, the **β3**- and **S3**-grafted colloids show average particle sizes around 140 nm (Table 1). The same tendency is observed for template-free colloids. This increase in the average particle size does not only reflect the presence of anchored organic groups at the colloids' surface. Indeed, the maximum particle diameter increase in the case of SC10 functions would be about 4 nm. Therefore the average particle size increase is attributed to a modification of the colloids' surface reactivity after grafting, which leads to the adsorption of solvent molecules, which, in return, increases their hydrodynamic diameter. This effect is well known for silica colloids.[14] The stability of the final colloidal suspensions will enable the use of conventional spectroscopic techniques to study the particles grafted with rhodamine-labeled peptides.

SEM of the samples before and after functionalization (Figure 2) does not show morphological differences between the as-prepared and grafted samples. As these observations are performed on dry particles, sizes derived by this measurement do not take into account any adsorbed solvent crown. Therefore, the particle sizes observed by SEM can be considered as bulk (or core) sizes and are not in contradiction with those measured by DLS.

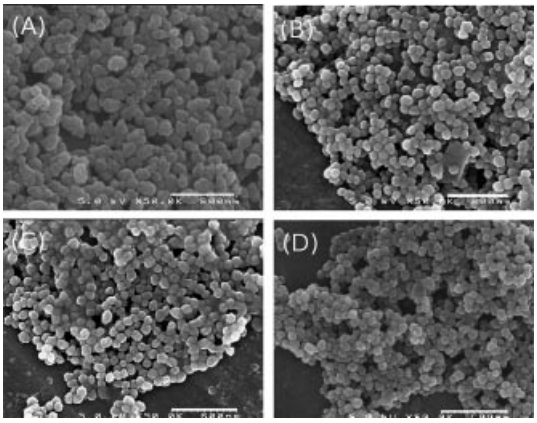

Figure 2. SEM micrographs of silicalite nanoparticles at various steps of the preparation: (A) as-synthesized **S** colloids, (B) **S3** particles, (C) tf-**S3** particles, and (D) tf-**S10** suspensions. Scale bar: 600 nm.

Microporosity

In order to follow the influence of the various treatments on the porous characteristics of the zeolite samples, nitrogen gas sorption analyses were performed on the as-synthesized nanoparticles and the grafted nanoparticles. The zeolite microporosity is revealed by N_2 adsorption on template-free samples (ca. 0.2 $cm^3 \cdot g^{-1}$) and the specific surface area

Table 1. DLS, N_2 adsorption/desorption, and elemental analysis data obtained for the as-synthesized, calcined, and grafted particles.

	Average diameter [nm ± 5%]	Specific area [$m^2 \cdot g^{-1}$]	Micropore volume [$cm^3 \cdot g^{-1}$]	% N	% C	Loading[a] [$\mu mol \cdot g^{-1}$]	Loading[b] [$\mu mol \cdot g^{-1}$]
β	57	224	0.098	1.65	12.50	0	0
β3	114	168	0.044	3.65	14.55	1.2	476
tf-**β**	62	439	0.142	0	0	0	0
tf-**β3**	163	223	0.082	2.61	8.27	2	621
S	64	75	0	0.76	9.85	0	0
S3	145	80	0	1.6	10.74	0.6	200
tf-**S**	–	505	0.155	0	0	0	0
tf-**S3**	145	370	0.107	1.48	4.31	2.4	352
tf-**S10**	147	217	0.056	1.17	7.98	1.5	278

[a] Theoretical values. [b] Measured from elemental analysis.

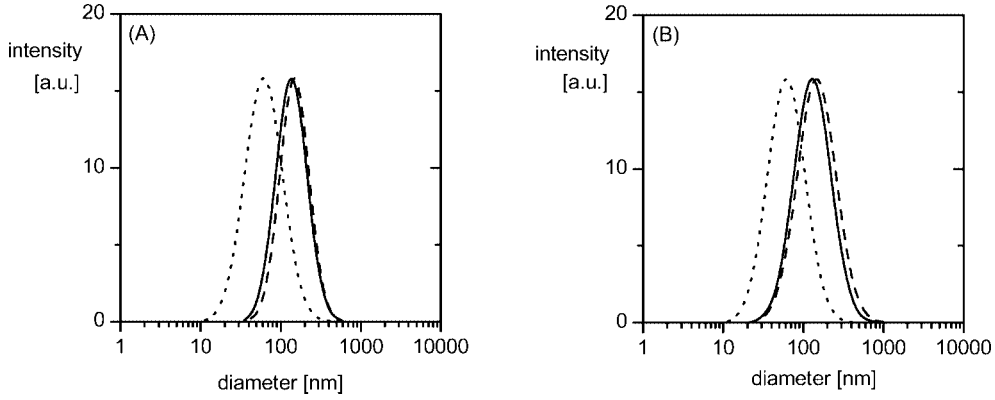

Figure 1. DLS profiles of silicalite nanoparticles at various steps of the preparation: (A) as-synthesized **S** colloids (dotted line), **S3** particles (solid line), and **S10** suspensions (dashed line); (B) as-synthesized **S** colloids (dotted line), tf-**S3** particles (solid line), and tf-**S10** suspensions (dashed line).

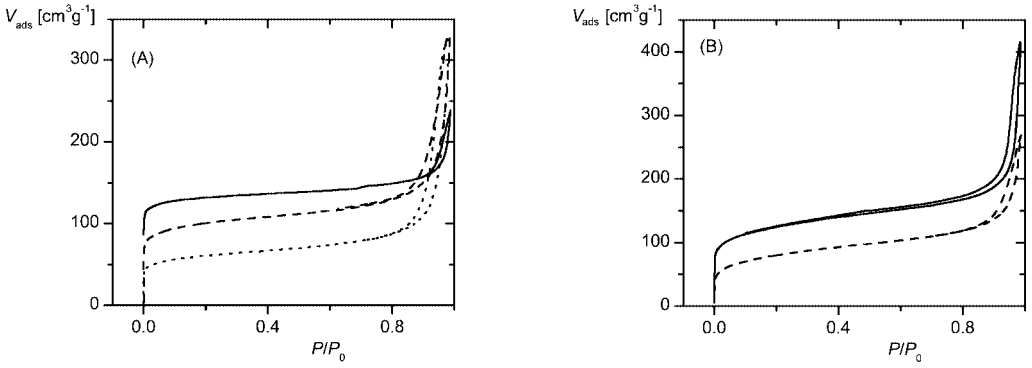

Figure 3. N_2 adsorption isotherms of silicalite nanoparticles (A) and zeolite β colloids (B): tf-**S** and tf-**β** (solid line), tf-**S3** and tf-**β3** (dashed line), tf-**S10** (dotted line).

is dramatically increased (ca. 3 times that of the as-synthesized samples) (Table 1). Grafting the zeolite nanoparticles, regardless of the structure used (β or silicalite-1), slightly decreases the specific surface area of the template-free sample (Table 1, Figure 3). This decrease of the micropore volume may indicate that some part of the grafting occurs inside the micropores. However, this decrease of the micropore volume is also observed for silane **1b**-grafted silicalite (tf-**S10** samples), although the size of this molecule forbids its entry through the pores. Therefore, the decrease of the measured micropore volume may be due to a decrease of its accessibility to N_2 (because of the presence of functional groups) instead of an actual decrease.

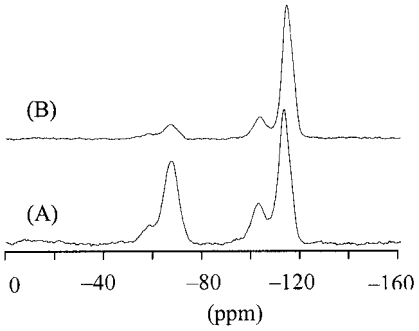

Figure 4. ^{29}Si CP-MAS NMR spectra recorded for **S3** (A) and **S10** (B) samples.

Grafting Quantification

Elemental analysis (N and C) allowed determination of the loading of the nanoparticles after the grafting procedure (Table 1). Assuming that each grafted silane molecule occupies 24 Å^2, the theoretical loading for a monolayer ranges between 0.55 and 2.4 mmol·g^{-1} depending on the specific surface area of the particles (Table 1).[15–18] As the experimental loading is below a monolayer coverage for each sample, this shows that the microporosity of the nanoparticles is not accessible for silanes **1a** and **1b**.

Grafting Analysis

CPMAS ^{29}Si NMR spectra of **S3** and **S10** nanoparticles present signals at δ = –101 and –110 ppm (Figure 4). Around –110 ppm, the overlapping resonances for both samples are assigned to zeolite framework silicon atoms. Resonances around –113/–115 ppm and –109/–110 ppm are assigned to *Si*(OSi)$_4$, Q4 species with minor resolution of the crystallographic sites. The signal at δ = –100 ppm is assigned to *Si*(OSi)$_3$OH, Q3 species.[19] The presence of a signal between –60 and –70 ppm indicates that silane **1** is covalently linked to the zeolite framework silicon atoms. Two resonances are observed corresponding to Si attached to the organic chain in two different chemical environments [–67 ppm: C–*Si*–(OSi)$_3$, T3 and –60 ppm: C–*Si*–(OSi)$_2$OH, T2 species].[20]

The presence of T2–T3 species, the absence of T1, C–*Si*(OSi)(OH)$_2$ and Q2, *Si*(OSi)$_2$(OH)$_2$ species and finally the variation in signal intensity for species Q3 and Q4 relative to bare particles demonstrated the efficient grafting of silane **1** on the surface of **S3** and **S10** nanoparticles. Spectra recorded on samples **S3** and **S10** present significant differences in the relative intensity of these characteristic resonances. Although, in the case of CP-MAS spectra, the peak intensity is not directly proportional to the species abundance, this intensity difference may reflect a greater grafting loading for silane **1a** than silane **1b**. This is a further confirmation of the elemental analysis results, which gave a higher coverage for a functionalization with silane **1a** than silane **1b**.

The CPMAS ^{13}C spectrum of **S3** nanoparticles presents three resonances situated at 9.7, 22.7 and 42.9 ppm corresponding to the propyl chain of silane **1a** (Figure 5). The additional resonance at δ = 162.1 ppm is attributed to the carbonyl group of the semicarbazide function. Signals corresponding to ethoxy groups or fluorenylmethoxycarbonyl (Fmoc) groups were not detected. This indicates the completion of the grafting reaction and the quality of the centrifugation–redispersion procedure.

^{29}Si and ^{13}C MAS NMR characterization of zeolite β nanoparticles leads to similar spectra presenting the characteristic resonances of T species around –60 ppm for ^{29}Si spectra and the carbonyl resonance at –162 ppm for ^{13}C spectra.

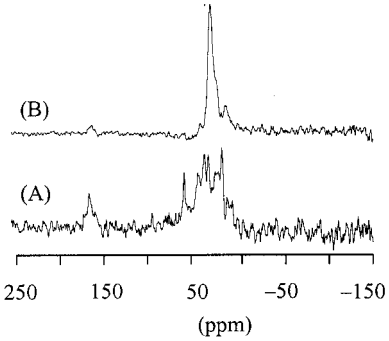

Figure 5. ^{13}C CP-MAS NMR spectra recorded for **S3** (A) and **S10** (B) samples.

Fluorescence Analysis

The nature of the interaction of peptides **2** and **3** with substrates **S**, **β**, **β3**, tf-**β3**, **S3**, and tf-**S10** was analyzed by fluorescence spectroscopy.

First, we checked the eventuality of nonspecific adsorption of peptides **2** and **3** on bare nanoparticles of zeolite **β** and silicalite **S**. After mixing peptides **2** and **3** with zeolite **β** nanoparticles, an intense fluorescence is observed (Figure 6). Meanwhile, very weak fluorescence intensity is obtained for samples based on silicalite **S** (Figure 6). Therefore, this indicates that the zeolite **β** surface is able to immobilize peptides by noncovalent interactions. This physisorption phenomenon is attributed to the presence of aluminum atoms at the zeolite **β** surface, which have been reported to present an affinity for peptides.[21] Fluorescence spectra registered on functionalized samples, **β3** and tf-**β3** treated with peptides **2** and **3**, presented an intense fluorescence for all samples, regardless of the peptide's nature (Figure 7). Therefore, interactions between peptides **2** or **3** and the zeolite **β** surface occurred even after surface modification. Indeed, as the fluorescence intensity observed for samples prepared with peptide **3** is higher than that obtained with peptide **2**, nonspecific adsorption is a highly probable phenomenon for samples based on zeolite **β**.

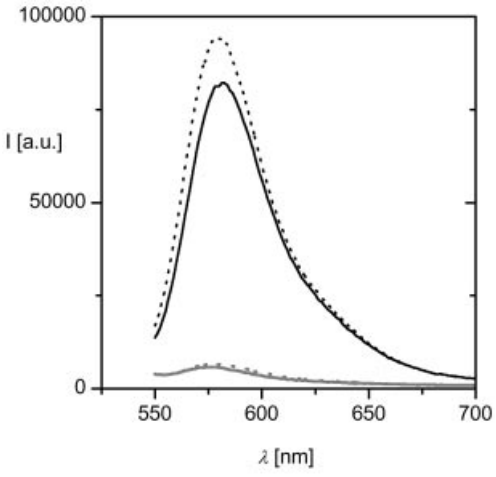

Figure 6. Fluorescence emission spectra of samples obtained after reaction between peptides **2** (dotted line) and **3** (solid line) with nanoparticles of zeolite **β** (black lines) and silicalite **S** (gray lines).

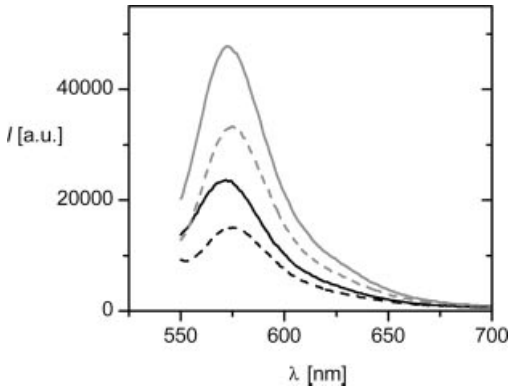

Figure 7. Fluorescence emission spectra of samples obtained after reaction between peptides **2** (dotted line) and **3** (solid line) with nanoparticles of zeolite **β3** (black lines) and tf-**β3** (gray lines).

By contrast, fluorescence spectra obtained with silicalite-based samples indicate a higher level of chemoselectivity. Therefore, for all these silicalite-based samples, the extent of physisorption was low and immobilization occurred mainly through the formation of a covalent bond between the semicarbazide groups on the surface and the α-oxo aldehyde group on the peptide molecule (Figure 8 and Figure 9). Fluorescence intensity ratio between samples **S3** obtained with peptide **3** and **2** (**S3-2/S3-3**) is around 40, showing that noncovalent interactions are rare with silicalite **S** (Figure 9).

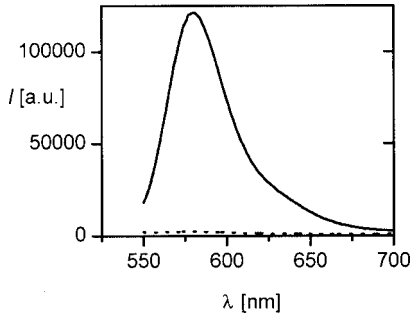

Figure 8. Fluorescence emission spectra of samples obtained after reaction between peptides **2** (dotted line) and **3** (solid line) with nanoparticles **S3**.

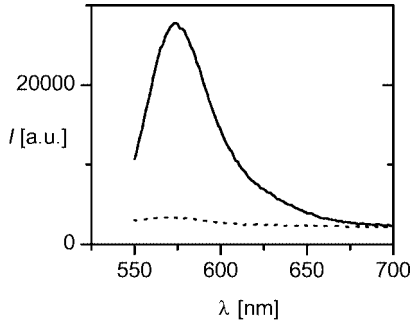

Figure 9. Fluorescence emission spectra of samples obtained after reaction between peptides **2** (dotted line) and **3** (solid line) with tf-**S10** nanoparticles.

A similar fluorescence intensity ratio is obtained with tf-**S10** samples reacted with peptide **3** and **2** (Figure 9). Therefore, this demonstrates that whatever the micropore volume or the spacer length of the silicalite substrate, COCHO-modified polypeptides are specifically and covalently immobilized on silicalite surfaces.

Comparison of fluorescence spectra obtained for **S3**, tf-**S3**, and tf-**S10** samples of identical concentrations indicates a lower fluorescence intensity for tf-**S10** samples (Figure 10). This may be attributed to the lower loading obtained for these samples for silane **1b** than silane **1a** (Table 1).

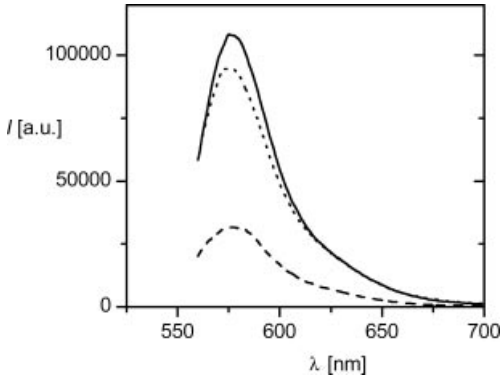

Figure 10. Fluorescence emission spectra of samples obtained after reaction between peptide **3** and **S3** (solid line), tf-**S3** (dotted line), and tf-**S10** nanoparticles (dashed line).

Conclusions

Monodisperse zeolite nanoparticles have been used to develop colloids bearing polypeptides anchored on the solid surface by a site-specific ligation method, which enables the control of the biomolecule orientation at the solid–liquid interface.

Two types of nanoparticles were studied: zeolite β, which possesses a Si/Al ratio of 25, and silicalite-1, which is a fully silicic material.

Fluorescence spectroscopy results demonstrated that the specificity of the ligation is dramatically influenced by the chemical composition of the particles' surface. Indeed, while zeolite β (aluminosilicate) particles react by nonspecific adsorption with the peptides, silicalite particles (pure silicate) anchor exclusively a peptide bearing the COCHO functionality. This particular physisorption phenomenon of zeolite β is attributed to the aluminum atoms present at the particles' surface, which have a specific affinity for peptides.

These materials could find applications in immunodiagnostics and drug delivery.

Experimental Section

Chemicals were purchased from commercial sources. They were reagent grade and used as received. Distilled deionized water (18 MΩ) was used for the preparation of all aqueous solutions.

Nanoparticle Preparation

Preparation of Colloidal Zeolite Nanoparticles: Colloidal zeolite β nanoparticles with a Si/Al ratio of 18.5 were synthesized under mild hydrothermal conditions from a clear solution containing $0.28Na_2O/9.0(TEA)_2O/0.5Al_2O_3/25SiO_2/430H_2O$, where TEA is tetraethylammonium hydroxide, the structure directing agent (SDA) (Fluka, 20% in water). The synthesis was performed at 100 °C for 8 days. Colloidal zeolite β crystals were purified by a series of high-speed centrifugation and ultrasonic redispersion in water or ethanol.

Colloidal silicalite-1 nanoparticles were synthesized under mild hydrothermal conditions from a clear solution containing $9.0(TPA)_2O/25SiO_2/295H_2O$, where TPA is tetrapropylammonium hydroxide, the structure directing agent (SDA) (Fluka, 20% in water). The synthesis was performed at 100 °C for 24 h. Colloidal silicalite-1 crystals were purified by a series of high-speed centrifugation and ultrasonic redispersion in water or ethanol.

Template-free colloidal silicalite and zeolite β nanoparticles were obtained by using a procedure described previously.[22] This approach is based on surface-grafted organic ligands, for example (2-aminoethyl)phoshonic acid (APA) $[H_2N(CH_2)_2PO(OH)_2$ from Fluka, or (3-aminopropyl)triethoxysilane (APTS) $[H_2N(CH_2)_3Si(OC_2H_5)_3$, ABCR]. These compounds are used as aggregation inhibitors and crystallinity stabilizers during high-temperature combustion of SDA. The grafting and subsequent calcination processing has no influence on size, morphology, and crystallinity of the zeolite nanoparticles. This procedure provides stable colloidal template-free monodisperse zeolite nanoparticles with particle size distribution similar to the initial colloid.

Semicarbazide Grafting of the Nanoparticles

We have recently described the preparation of semicarbazide-functionalized monodisperse silica ludox nanoparticles.[23] The same strategy was adopted here for each type of porous nanoparticle (silicalite and zeolite β). (Scheme 1).

First, silanes **1** were synthesized by reacting (3-isocyanatopropyl)- or (10-isocyanatodecyl)triethoxysilane[13] with $FmocNHNH_2$.[24] Then, silanes **1** were reacted as shown in Scheme 1, on the nanoparticles. The grafting of semicarbazide functionality was performed in DMF using silane **1** (3 mmol·g^{-1}) in the presence of piperidine, which permitted the in situ removal of the Fmoc-protecting group and improved the silanization process.[26] The nanoparticles were washed with DMF by centrifugation and stored at 4 °C, 1% (w/v) in DMF. The suspensions were found to be stable for months.

Peptide Grafting of the Nanoparticles

The nanoparticles were then reacted with peptides **2** and **3** labeled with (5)-6-carboxymethylrhodamine. Detailed synthesis of the peptides has been reported elsewhere.[25] The peptide grafting (1 mL, 0.5–1 mM) was performed in acetate buffer (100 mM, pH = 5.51) at 37 °C. The excess of peptide was eliminated by five cycles of centrifugation (11000 rpm, 20 min). The final water suspension [1% (w/v)] was stored at 4 °C.

As peptide **2** bares a COCHO functionality, it should react with the semicarbazide surface, whereas immobilization of peptide **3**, which lacks the COCHO, should occur only through physisorption (Scheme 2).

Sample Characterization

Nanoparticle Size: The mean particle size was determined by dynamic light scattering (DLS) using an argon laser (Spectra Physics Series 2000) operating at 632.8 nm. Light-scattering measurements

were made at 25 ± 0.1 °C. Hydrodynamic measurements were performed at a 90° angle, after dilution of the sample to 10 μg·mL^{-1} in water. The data were analyzed according to the method of cumulants for apparent mean diameter and polydispersity index.[26]

Nanoparticle Morphology: The morphology of the nanoparticles was investigated by scanning electron micrography (SEM, Hitachi S-4500) and transmission electron microscopy (TEM, JEOL 1200 EX with 120 keV accelerating voltage). SEM samples were prepared by depositing colloidal suspension on platinum-coated (2–3 nm) aluminum mounts fixed with carbon conducting tape. TEM samples were prepared by depositing 5 μL of silica nanoparticles water suspension (diluted 1:20) on 300 mesh copper grid with carbon film backing.

Nanoparticle Microstructure: The microstructure was studied by gas sorption experiments (Micromeretics ASAP 2010). Nitrogen was used as the adsorbate at 77 K. Samples were outgassed at 80 °C in dynamic vacuum (3×10^{-6} bar) before the adsorption. Determination of the specific surface was done by the BET method and total micropore volume was obtained by t-plot method based on the Harkins-Jura equation.

Nanoparticle Grafting: The nature of the functionalization was studied with ^{29}Si and ^{13}C CP-MAS NMR performed on the samples after each step of the preparation procedure. ^{29}Si solid-state NMR spectroscopy gave useful information on the silanization step, as the chemical shift of ^{29}Si was highly sensitive to number and nature of groups attached to it. ^{29}Si CP-MAS NMR spectra of the solid samples were recorded with a Bruker spectrometer at 79.49 MHz using 5-μs single pulses (60° flip angle) with 10-s repetition rate and 15-ms contact time employing magic angle spinning at 3.5 kHz; 10000 scans were accumulated. All ^{29}Si chemical shifts were referenced to tetramethylsilane (TMS). ^{13}C CP-MAS NMR spectra were recorded with a Bruker spectrometer at 100.62 MHz using 10-μs single pulses (π/6) with 5-s repetition rate and 3-ms contact time employing magic-angle spinning at 3.5 kHz; 50000 scans were accumulated.

The powder samples were filled into 4-mm diameter zirconia rotors.

Elemental Analysis: Elemental analysis by the "Laboratoire Central d'Analyses du CNRS", Vernaison (France) enabled the evaluation of the grafting loading after functionalization.

Photophysical Properties: The optical properties of the particles were evaluated by recording static fluorescence spectra using a Spex Fluorolog 1681 spectrofluorimeter (scanning rate of 2 nm·s^{-1}). Spectra were recorded on 0.05% w/w particle suspensions.

Acknowledgments

Funding of this work by the Ministère Délégué à la Recherche (ACI Nanosciences 045 270 and 042 130) is gratefully acknowledged. The authors thank Grace-Davidson for generously providing Ludox silica samples for the zeolite synthesis.

[1] C. M. Niemeyer, *Angew. Chem. Int. Ed.* **2001**, *40*, 4128–4158.
[2] N. L. Rosi, C. A. Mirkin, *Chem. Rev.* **2005**, *105*, 1547.
[3] T. Pellegrino, S. Kudera, T. Liedl, A. Muñoz Javier, L. Manna, W. J. Parak, *Small* **2005**, *1*, 48–63.
[4] *Chem. Mater.*, special issue on organic–inorganic nanocomposite materials, **2001**, *13*, 3059–3809.
[5] S. Onclin, B. J. Ravoo, D. N. Reinhoudt, *Angew. Chem. Int. Ed.* **2005**, *44*, 6282–6304.
[6] I. Lukěs, M. Borbaruah, L. D. Quin, *J. Am. Chem. Soc.* **1994**, *116*, 1737.
[7] R. D. Badley, W. T. Ford, F. J. McEnroe, R. A. Assink, *Langmuir* **1990**, *6*, 792.
[8] L. Tosheva, V. Valtchev, *Chem. Mater.* **2005**, *17*, 2494–2513.
[9] B. Wheatley, D. E. Schmidt Jr, *J. Chromatogr. A* **1999**, *849*, 1–12.
[10] W. Clarke, J. D. Beckwith, A. Jackson, B. Reynolds, E. M. Karle, D. S. Hage, *J. Chromatogr. A* **2000**, *888*, 13–22.
[11] B. Lu, J. Xie, C. Lu, C. Wu, Y. Wie, *Anal. Chem.* **1995**, *67*, 83–87.
[12] A. Vijayendran, D. E. Leckband, *Anal. Chem.* **2001**, *73*, 471–480.
[13] P. Joly, N. Ardès-Guisot, S. Kar, M. Granier, J.-O. Durand, O. Melnyk, *Eur. J. Org. Chem.* **2005**, *12*, 2473–2480.
[14] R. K. Iler, *The Chemistry of Silica*, Wiley, New York, NY, **1979**.
[15] A. Y. Fadeev, T. J. McCarthy, *Langmuir* **1999**, *15*, 3759–3766.
[16] A. Y. Fadeev, T. J. McCarthy, *Langmuir* **2000**, *16*, 7268.
[17] M. J. Stevens, *Langmuir* **1999**, *15*, 2773–2778.
[18] S. Pawsey, K. Yach, L. Reven, *Langmuir* **2002**, *18*, 5205–5212.
[19] G. Engelhardt, D. Michel, *High Resolution Solid-State NMR of Silicates and Zeolites*, Wiley, New York, NY, **1987**.
[20] G. S. Caravajal, D. E. Leyden, G. R. Quinting, G. E. Macial, *Anal. Chem.* **1988**, *60*, 1776.
[21] M. V. Graf, B. Saegesser, G. A. Schoenenberger, *Anal. Biochem.* **1986**, *157*, 295.
[22] M. Smaïhi, E. Gavilan, J.-O. Durand, V. Valtchev, *J. Mater. Chem.* **2004**, *14*, 1347–1351.
[23] O. El-Mahdi, X. Duburcq, C. Maillet, C. Olivier, J. M. Garcia, J. O. Durand, O. Melnyk, *Anal. Chem.*, manuscript submitted.
[24] E. Zhang, Y. L. Cao, M. W. Hearn, *Anal. Biochem.* **1991**, *195*, 160–167.
[25] C. Olivier, D. Hot, L. Huot, N. Ollivier, O. El-Mahdi, C. Gouyette, T. Huynh-Dinh, H. Gras-Masse, Y. Lemoine, O. Melnyk, *Bioconjugate Chem.* **2003**, *14*, 430–439.
[26] D. E. Koppel, *J. Chem. Phys.* **1972**, *57*, 4814.

Received: February 27, 2006
Published Online: May 18, 2006

